JOURNAL OF ENGINEERING SCIENCES

Volume 7, Issue 2 (2020)

Hu W. J. (2020). Effects of metal particles on cold spray deposition onto Ti-6Al-4V alloy via Abaqus/Explicit. Journal of Engineering Sciences, Vol. 7(2), pp. E19–E25, doi: 10.21272/jes.2020.7(2).e4

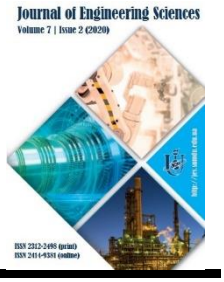

Effects of Metal Particles on Cold Spray Deposition onto Ti-6Al-4V Alloy via Abaqus/Explicit

Hu W. J.

[1] National Aerospace University "Kharkiv Aviation Institute", 17, Chkalova St., 61000 Kharkiv, Ukraine;
[2] School of Aeronautics and Astronautics, Nanchang Institute of Technology, Jiangxi, Nanchang, Qingshanhu District, China

Article info:
Paper received: September 21, 2020
The final version of the paper received: December 7, 2020
Paper accepted online: December 13, 2020

***Corresponding email:**
837406613@qq.com

Abstract. Titanium alloy is the main structural material of the aerospace system component. About 75 % of titanium and titanium alloys in the world are used in the aerospace industry. Hence, it is of great significance to study the surface deposition characteristics by cold spraying technology, taking Ti-6Al-4V alloy as an example, smoothed particle hydrodynamics (SPH) method in Abaqus/Explicit was used to spray aluminum, Ti-6Al-4V, copper, tungsten alloy (W alloy) and titanium particles onto Ti-6Al-4V substrate. The simulation results show that the deposition effect is good over 600 m/s, and higher energy is obtained for Ti-6Al-4V particles with the same properties as the matrix. For aluminum, Ti-6Al-4V, copper, W alloy, and titanium particles with different properties, under the same initial speed condition, the greater the density of the material, the deeper the foundation pit. W Alloy has the largest initial kinetic energy, the deepest foundation pit, and better surface bonding performance. The aluminum particle has the smallest initial kinetic energy, the shallowest foundation pit. However, the deposition effect of multiple aluminum particles has not improved. The collision process's kinetic energy is transformed into internal energy, frictional dissipation, and viscous dissipation. Besides, the internal energy is mainly plastic dissipation and strain energy. Therefore, it is recommended to use Ti-6Al-4V, copper, nickel, W alloy, and titanium particles for different occasions, such as Ti-6Al-4V substrate surface restorative and protective coatings. Pure aluminum particles are not recommended.

Keywords: cold spraying technology, smoothed particle hydrodynamics, tungsten alloy, aerospace industry.

1 Introduction

Ti-6Al-4V alloy is widely used in aerospace and has the advantages of high specific strength, good corrosion resistance, and high-temperature resistance [1, 2]. However, its low wear resistance limits the further development of titanium alloy. Besides, its high manufacturing cost, if only require the occasion of surface performance, can reduce the substrate's use and then reduce the cost.

Surface-repaired titanium alloy parts by cold spraying technology are good ways to solve those problems [3]. Cold Spraying (CS) [4] technology was new in recent years, which is mainly applied for surface repair and protection of coating or additive manufacturing applications [5, 6]. At a supersonic velocity by Laval nozzle, particles impact and plastically deform on the substrate. The deformation process results in adhesion to the surface.

In this paper, the Abaqus/Explicit method was used to spray aluminum, copper, Ti-6Al-4V, titanium, and tungsten alloy onto Ti-6Al-4V substrate to study the effects of different metal particle properties.

2 Research Methodology

2.1 Model and method

The Abaqus/Explicit method includes three algorithms, ALE (arbitrary Lagrangian-Eulerian), CEL (Couple Lagrangian-Eulerian), SPH (Smoothed Particle Hydrodynamics). This paper uses the SPH method, a meshless method that has been gradually developed in the past twenty years. Its advantage lies in avoiding mesh distortion during large deformations.

Besides, the SPH method belongs to the Lagrange algorithm. Compared with the Euler method, it does not need to discretize the empty area, saving a lot of internal storage and calculation time. Hence, the SPH method is very suitable for dealing with various large deformation and fluid-structure coupling problems. The unit type of the model is a hexahedral element (C3D8R). The deposition time of supersonic cold aerodynamic spraying is short, and the strain rate is significant.

Therefore, the material model needs to consider parameters such as plasticity, friction, damage. Hence, the J-Cook plastic model [7–9] was used:

$$\sigma = \left[A + B\varepsilon_{\mathrm{p}}^{\mathrm{n}}\right]\left[1 + C\ln\left(\frac{\dot{\varepsilon}_p}{\dot{\varepsilon}_0}\right)\right]\left[1 - \left(T^*\right)^{\mathrm{m}}\right] \quad (1)$$

where σ is the equivalent flow stress; $\dot{\varepsilon}_p$ and $\dot{\varepsilon}_0$ are equivalent plastic strain rate and reference strain rate; ε_p is equivalent plastic strain; parameters A, B, C, n, and m are material constants; T^* is the normalized temperature:

$$T^* = \begin{cases} 0; & T < T_{\mathrm{trans}} \\ (T - T_{\mathrm{trans}})/(T_{\mathrm{melt}} - T_{\mathrm{trans}}); & T_{\mathrm{trans}} \le T \le T_{\mathrm{melt}} \\ 1 & T_{\mathrm{melt}} \le T \end{cases} \quad (2)$$

where T_{melt} is the melting temperature; T_{trans} is a reference transition temperature at or below which there is no temperature dependence of the response [10].

The calculation finite-element model is presented in Figure 1.

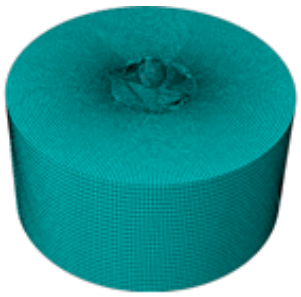

Figure 1 – The calculation finite-element model

The main parameters of the simulation process are shown in Table 1.

Table 1 – Material parameters of aluminum, copper, Ti-6Al-4V, titanium, and tungsten alloy

Material	Aluminum	Copper	Ti-6Al-4V	Titanium	Tungsten alloy
Density ρ, g/cm^3	2.70	8.90	4.50	4.54	17
Poisson's ratio, ν	0.33	0.35	0.30	0.30	0.30
Yield strength A, MPa	148.4	90	862	175	790
Hardening index B, MPa	345.5	292	331	380	510
Strain index, N	0.183	0.31	0.34	0.32	0.27
Softening index, M	0.895	1.09	0.8	0.55	1.05
Strain rate, C	0.001	0.025	0.014	0.060	0.016
d_1	0.071	0.54	–0.09	–0.09	3
d_2	1.248	4.89	0.25	0.27	0
d_3	1.142	3.03	–0.5	0.48	0.78
d_4	0.147	0.014	0.014	0.014	0
d_5	1.00	1.12	3.87	3.87	0
Shear modulus, MPa	27.0	44.7	59.6	44	77
Specific heat Cp, J/(kg·K)	898.2	383	612	452	134
Thermal conductivity coefficient λ, W/(m·K)	237.2	386.5	7.955	16.3	170
Melting temperature T_m, °C	916	1356	1878	1811	1800
Transformation temperature T_{trans}, °C	298	298	298	298	298

The material failure model used in this paper is the Johnson-Cook dynamic fracture model. Considering the influence of static pressure, strain rate, and temperature, it can be expressed in the following equation [11]:

$$\varepsilon_{\mathrm{f}} = \left[\mathrm{d}_1 + \mathrm{d}_2\exp\left(\mathrm{d}_3\frac{\mathrm{p}}{\mathrm{q}}\right)\right]\left[1 + \mathrm{d}_4\ln\left(\frac{\dot{\varepsilon}_{\mathrm{p}}}{\dot{\varepsilon}_0}\right)\right]\left(1 + \mathrm{d}_5 T*\right) \quad (3)$$

where ε_f is fracture strain, d_1 – d_5 are material fracture constants; p is static pressure; q is mises yield stress.

Besides, this paper uses the linear EOS_GRUNEISEN state equation as the material state equation:

$$U_S = C_0 + sU_P, \quad (3)$$

where C_0 and s define the linear relationship between the linear shock velocity U_S and the particle velocity U_P, the parameters as shown in Table 2.

Table 2 – US-UP state equation parameters of SPH simulation process

Materials	C_0, 10^6	S	Gamma$_0$
Aluminum	5.386	1.339	2.18
Copper	3.940	1.489	1.97
Ti-6Al-4V	5.130	1.028	1.23
Titanium	4.700	1.489	1.97
Tungsten alloy	3.990	1.240	1.54

2.2 Material properties

The material particles are spherical particles with a diameter of 10 μm and a Ti-6Al-4V matrix radius of 130 μm. Studies have shown in [12–14] show that the critical velocities of Ti-6Al-4V are in a range of 502–780 m/s. This paper utilizes 400, 600, 800, and 1000 m/s to collide with the Ti-6Al-4V substrate vertically. To further study the energy conversion process, 650 m/s is used to analyze energy for different particles.

3 Results and Discussion

3.1 Numerical simulation results

The numerical simulation results are presented in Figures 2–6.

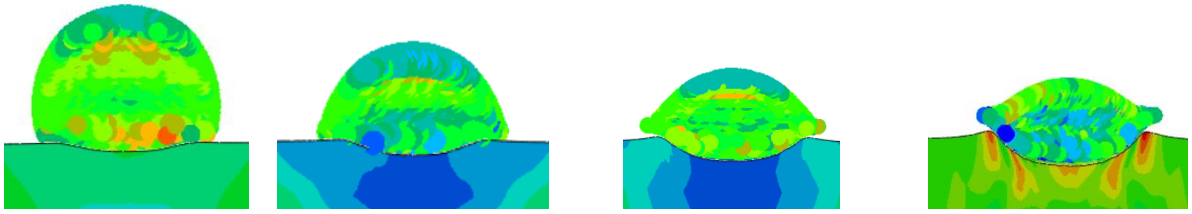

a b c d

Figure 2 – Ti-6Al-4V/Ti-6Al-4V within 50 ns: a – 400 m/s; b – 600 m/s; c – 800 m/s; d – 1000 m/s

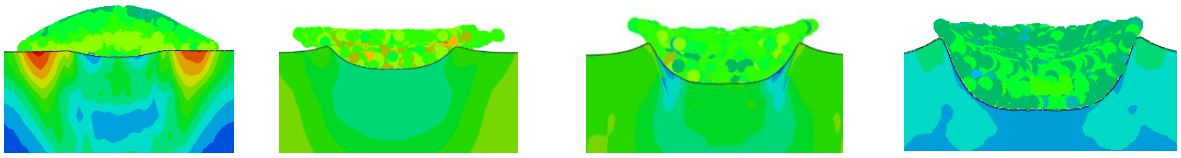

a b c d

Figure 3 – Copper/Ti-6Al-4V within 50 ns: a – 400 m/s; b – 600 m/s; c – 800 m/s; d – 1000 m/s

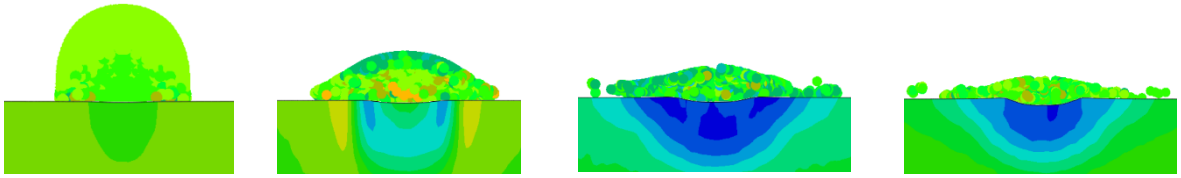

a b c d

Figure 4 – Aluminum/Ti-6Al-4V within 50 ns: a – 400 m/s; b – 600 m/s; c – 800 m/s; d – 1000 m/s

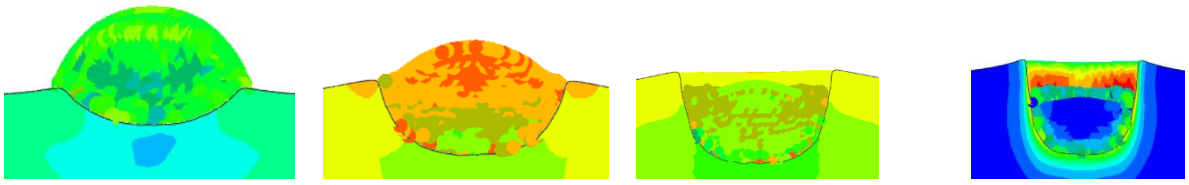

a b c d

Figure 5 – W alloy/Ti-6Al-4V within 50 ns: a – 400 m/s; b – 600 m/s; c – 800 m/s; d – 1000 m/s

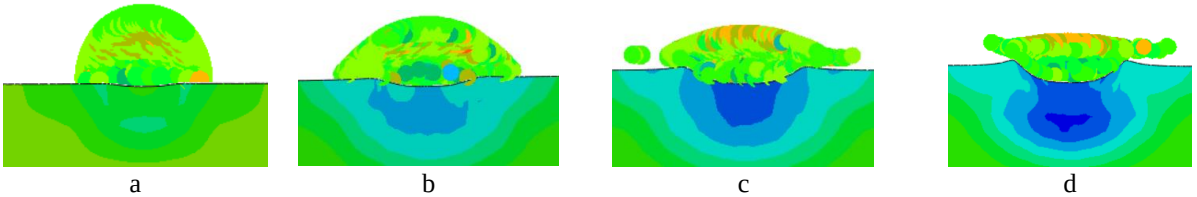

a b c d

Figure 6 – Titanium/Ti-6Al-4V within 50ns: a – 400 m/s; b – 600 m/s; c – 800 m/s; d – 1000 m/s

Ti-6Al-4V particle collides Ti-6Al-4V alloy is a hard material collision hard material. As Figure 2 b shows, the 600–800 m/s deposition effect is the best. When the particles exceed 1000 m/s, adiabatic shear instability begins to occur during the deposition process.

Copper particles collide Ti-6Al-4V titanium alloy is a hard material collision hard material. As figure 3(b) shows, the over 600 m/s deposition effect is good.

Aluminum particles collide with Ti-6Al-4V alloy, which is a soft material colliding with a hard material. It can be seen from Figure 4 b that the deposition effect is the best. The best deposition effect is around 600 m/s, but the foundation pit is very shallow. When the particle velocity reaches above 800 m/s, the particle fails and cannot be deposited effectively.

Figure 5 shows the tungsten alloy collide with the Ti-6Al-4V alloy substrate. The 400–600 m/s deposition effect is the best. When the particles exceed 800 m/s, foundation pit depth is deeper than other materials, and all erode into the Ti-6Al-4V matrix.

Titanium particles collide Ti-6Al-4V titanium alloy is a hard material collision hard material. Figure 6 b shows that the 600–800 m/s deposition effect is the best. When the particles exceed 800 m/s, adiabatic shear instability occurs during the deposition process. Besides, foundation pit depth is shallower than Ti-6Al-4V particles from 600 to 800 m/s.

From the energy view, as the energy evolution process is shown in Figure 7, where ALLAE is artificial strain energy, ALLFD is frictional dissipation, ALLIE is internal energy, ALLKE is kinetic energy (Figure 7 d), ALLPD is plastic dissipation, ALLSE is strain energy, and ALLVD is viscous dissipation. Take Ti-6Al-4V/Ti-6Al-4V (600 m/s) as the example. Artificial strain energy value (Figure 7 a) within 50 ns is very small and can be neglected.

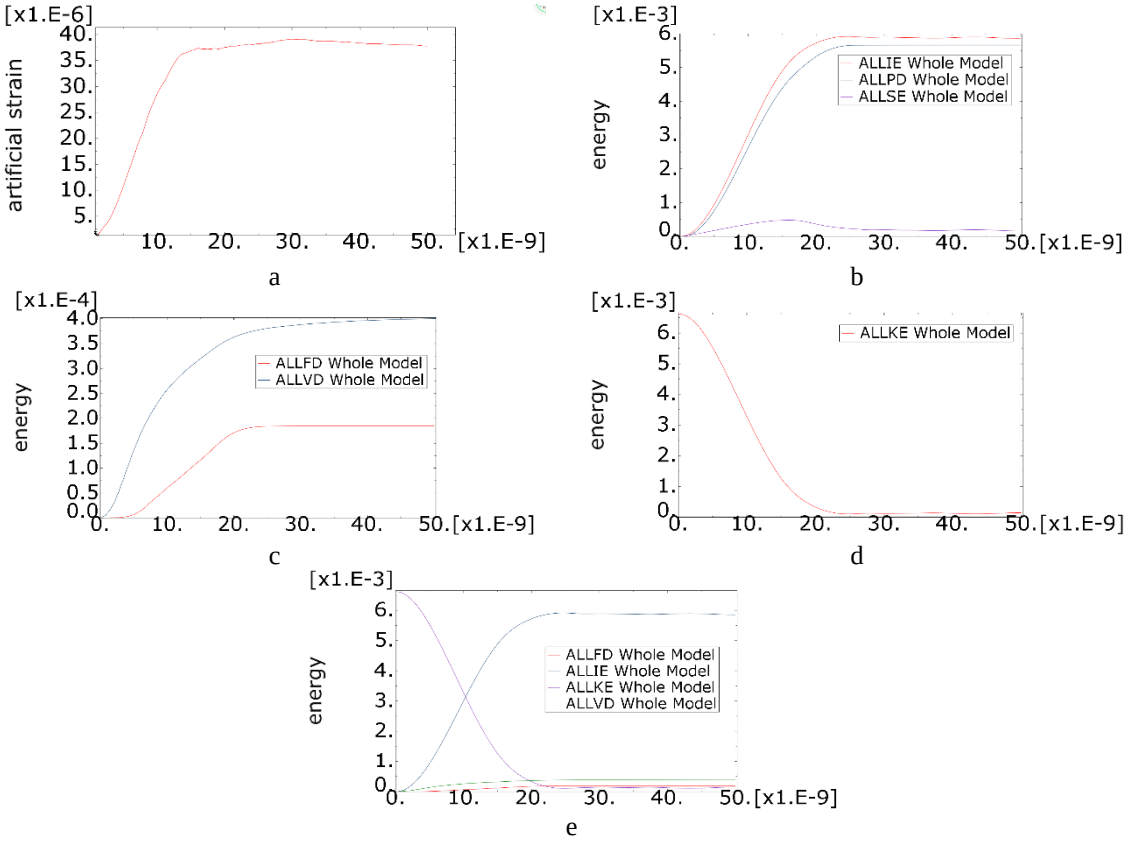

Figure 7 – Energy conversion curves of collision process within 50 nanoseconds: a – artificial strain energy; b – internal energy change process; c – frictional and viscous dissipation energy; d – kinetic energy change process; e – energy change process of the whole model

As Figure 7 b shows, total strain energy "ALLIE = = ALLPD + ALLSE". However, there is also frictional dissipation and viscous material dissipation in the collision process (Figure 7 c). Hence, the final energy change process is shown in Fig. 7 e (the same below), which the formula is expressed as "ALLKE = ALLIE + + ALLFD + ALLVD".

Due to the difference in the particles' initial kinetic energy and energy conversion rate, the internal energy obtained by each substrate is also different. Figure 8 shows the energy transition process during the particle collision process. The results show that the initial particle when the velocity is the same, the denser particles have, the greater initial kinetic energy.

It can be seen from Figure 8, because the density of copper, Ti-6Al-4V, titanium and tungsten alloy is the larger than aluminum, the initial kinetic energy is the larger at the beginning of the collision. Internal energy of the substrate rise rapidly, causing the particles to be in contact, the temperature rises sharply, hence, it is easier to get a deeper foundation pit.

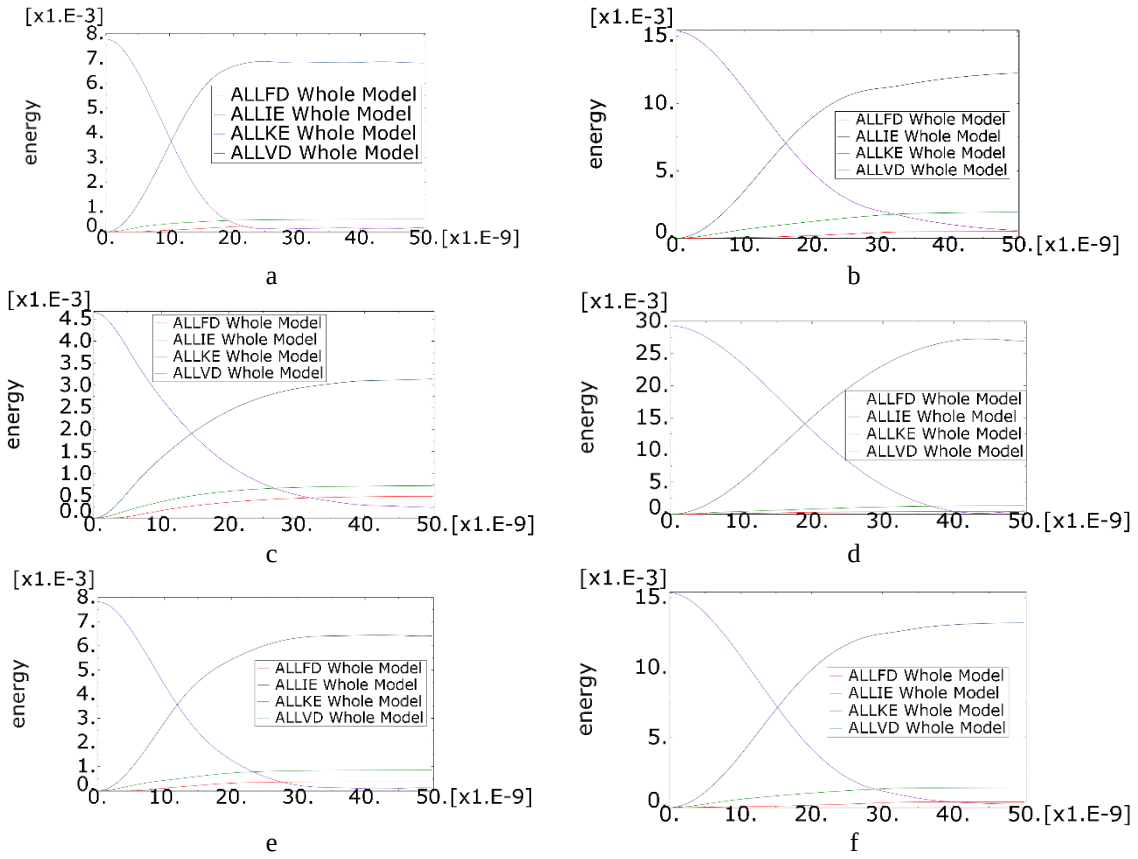

Figure 8 – Deposition velocity at 650 m/s with energy curve within 50 ns: a – Ti-6Al-4V/ Ti-6Al-4V; b – Copper/Aluminum/ Ti-6Al-4V; c – Aluminum/Ti-6Al-4V; d – W alloy/Ti-6Al-4V; e – Ti/Ti-6Al-4V; f – Nickel/Ti-6Al-4V

The Ti-6Al-4V matrix particles deposited on the surface of the Ti-6Al-4V substrate belong to the same material properties (Figure 8 a). Due to the larger specific heat capacity and low thermal conductivity, it is easier to absorb more energy, and the deposition effect is a better one, so it can finally get more energy.

As we know, Aluminum/Ti-6Al-4V belongs to soft material collision hard material, which has a small shear modulus. Hence, its foundation pit is shallow, and the bonding performance needs to be further studied. Besides, the internal energy (ALLIE) does not drop rapidly in the later stage, and it is still at a significant value. This is mainly due to the released energy of the accumulated plastic deformation process.

For verification, the fact that the initial kinetic energy is significant, the energy is considerable, and the deeper the foundation pit is, nickel particles are used for verification. Since the initial kinetic energy is related to the mass and initial speed, this article uses the same volume and the same speed to collide. The nickel foundation pit's simulation result should be more significant than the aluminum one is close to copper particles. As shown in Figure 9, it meets expectations.

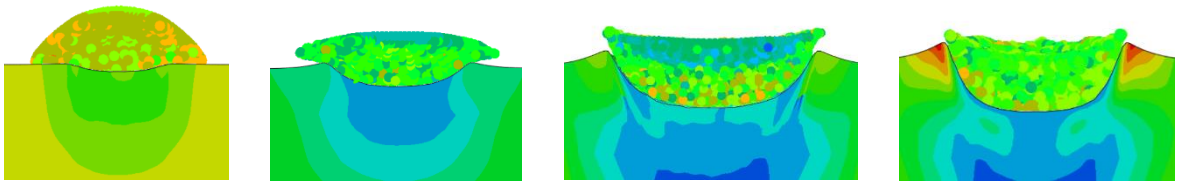

a b c d

Figure 9 – Nickel/Ti-6Al-4V within 50 ns: a – 400 m/s; b – 600 m/s; c – 800 m/s; d – 1000 m/s

3.2 Study of multi-particle aluminum collision with Ti-6Al-4V matrix

As shown above, a single copper, W alloy, nickel, titanium, and Ti-6Al-4V particles deposited on the surface of Ti-6Al-4V has a deep foundation pit effect of depositing Ti-6Al-4V on a single pure aluminum particle is not ideal.

The energy map shows that the initial energy of aluminum is small. For exploring whether the depth of the foundation pit is related to energy, a number of aluminum particles are studied. The model is shown in Figure 10.

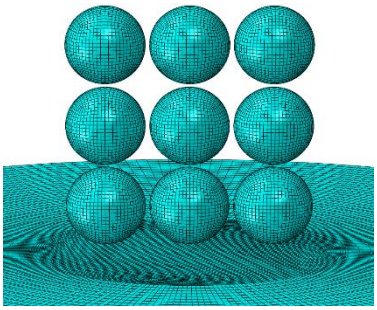

Figure 10 – The calculation model

Figures 11 and 12 show that multiple particles increase the initial kinetic energy. Although the subsequent particles have a compacting effect on the previous particles, the deposition effect is still not good. Hence, pure aluminum particles are not recommended for Ti-6Al-4V surface deposition. Further studies are needed for aluminum mixed with other particles for deposited onto Ti-6Al-4V.

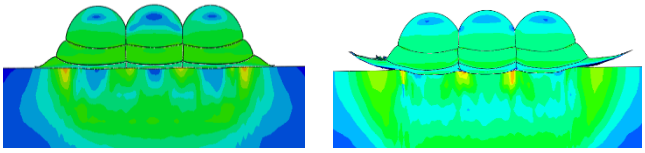

a b

Figure 11 – Multiple aluminum particles deposited onto titanium within 70 nanoseconds: a – 650 m/s; b – 650 m/s for the 1st-layer and the 2nd-layer particles, and 1000 m/s for the 3rd-layer particles are 1000 m/s

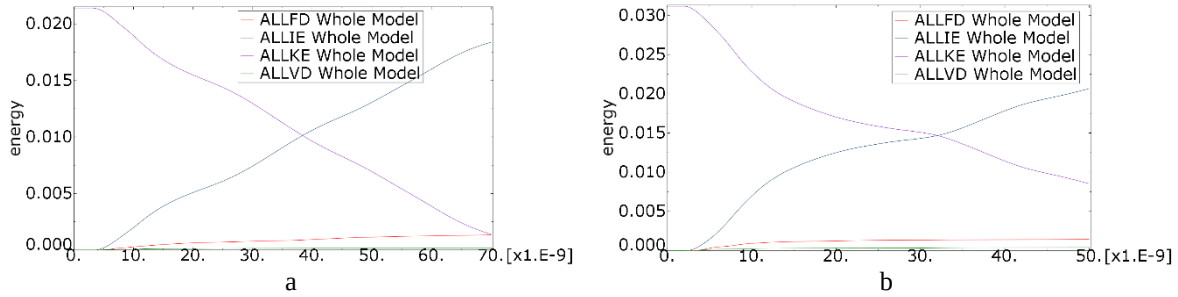

a b

Figure 12 – Energy diagram of multiple aluminum particles collide with the titanium surface within 70 ns: a – 650 m/s; b – 650 m/s for the 1st-layer and the 2nd-layer particles, and 1000 m/s for the 3rd-layer particles are 1000 m/s

4 Conclusions

The surface of the Ti-6Al-4V alloy substrate can be cold sprayed with aluminum, copper, W alloy, nickel, titanium, and Ti-6Al-4V particles. The impact deposition effect is mainly affected by material hardness, density, specific heat capacity, thermal conductivity. According to different particle deposition characteristics, for the Ti-6Al-4V substrate, it is recommended to use Ti-6Al-4V, nickel, copper, W alloy, and titanium particles as surface restorative, protective and functional coating materials, and pure aluminum particles are not recommended.

Compared with the hardness of the Ti-6Al-4V matrix, the particles with larger hardness in the collision process led to deeper foundation pits. For example, at a speed of 600 m/s, nickel particles deposit deeper pits than aluminum particles.

Particles with higher density have the more significant the initial kinetic energy, the better the deposition effect. For instant, the density of nickel particles (density is 8.9 g/cm^3) is higher than that of aluminum particles (density is 2.7 g/cm^3), the foundation pit is deeper during the deposition process. Hence, the bonding performance is better. Similarly, the foundation pit deposited by tungsten alloy is deeper than a nickel.

The energy conversion process of collision is mainly kinetic energy (ALLKE) conversion to internal energy (ALLIE), and a small part into frictional dissipation (ALLFD) and viscous dissipation (ALLVD). As the single-particle and multi-particle energy processes of aluminum particles show, the initial energy increase does not necessarily lead to better deposition, depending on the substrate's physical properties and particles.

5 Acknowledgments

The author would like to thank the China Scholarship Council for its support (No. 202008100011).

References

1. Loina, A., Rinner, M.; Alonso, F., Onate, J. I, Ensinger, W. (1998). Effects of plasma immersion implantation of oxygen on mechanical properties and microstructure of Ti6Al4V. *Surface and Coatings Technology*, Vol. 103, pp. 262–267, doi: 10.1016/S0257-8972(98)00411-3.
2. Jin, H. X., Wei, K. X., Li, J. M., Zhou, J. Y. (2015). Research development of titanium alloy in aerospace industry. *The Chinese Journal of Nonferrous Metals*, Vol. 35, pp. 280–292.
3. Hu, W. J., Markovych, S., Tan. K., Shorinov, O., Cao. T. T. (2020). Surface repair of aircraft titanium alloy parts by cold spraying technology. *Aerospace technic and technology*, Vol. 163, pp. 30–42, doi: 10.32620/aktt.2020.3.04.

4. Anatolii, N.P. (2007). *Cold Spray Technology*. Elsevier Publishing House, Netherlands.
5. Tan, K., Markovych, S., Hu, W. J., Shorinov, O., Wang, Y. R. (2020). Review of manufacturing and repair of aircraft and engine parts based on cold spraying technology and additive manufacturing technology. *Aerospace Technic and Technology*, Vol. 163, pp. 53–70, doi: 10.32620/aktt.2020.3.06.
6. MacDonald, D., Fernandez, R., Delloro, F., Jodoin, B. (2017). Cold spraying of Armstrong process titanium powder for additive manufacturing. *Thermal Spray Technology*, Vol. 26, pp. 598–609.
7. Assadi, H., Gartner, F., Stoltenhoff, T., Kreye, H. (2003). Bonding mechanisms in cold gas spraying. *Acta Materials*, Vol. 51, pp. 4379–4394, doi: 10.1016/S1359-6454(03)00274-X.
8. Johnson, G. R., Cook, W. H. (1983). A constitutive model and data for metals subjected to large strains, high strain rates, and high temperatures. *7th International Symposium on Ballistics Hague*, pp. 541–547.
9. Wu, X. K., Zhou, X. L., Cui, H., Zhang, J. S. (2012). Morphology prediction of cold sprayed Cu and Al coatings through multi-particles deposition simulation. *Journal of University of Science and Technology Beijing*, Vol. 34, pp. 1391–1399.
10. Bae, G., Xiong, Y., Kumar, S., Lee, C. (2008). General aspects of interface bonding in kinetic sprayed coatings. *Acta Materials*, Vol. 56, pp. 4858–4868, doi: 10.1016/j.actamat.2008.06.003.
11. Li, W. Y. (2009). 3-D FEM analysis of impacting behavior of cold sprayed particles. *China Surface Engineering*, Vol. 22, pp. 31–37.
12. Sunday, T. O.; Jen, T. C. (2019). A comparative review on cold gas dynamic spraying processes and technologies. *Manufacturing Review*, Vol. 25, pp. 1–20, doi: 10.1051/mfreview/2019023.
13. Pelletier, J. L. (2013). Development of Ti-6Al-4V coating onto Ti-6Al-4V substrate using low pressure cold spray and pulse gas dynamic spray. *The University of Ottawa*, doi: 10.20381/ruor-4265.
14. Jin, L.; Cui, X. Z.; Ding, Y. F.; Zhang, L.; Su, X. D. (2017). Critical deposition velocity calculations and properties investigations of TC4 cold spray coatings. *Surface Technology*, Vol. 46, pp. 96–101, doi: 10.16490/j.cnki.issn.1001-3660.2017.08.016.